Contributed paper

OPTO-ELECTRONICS REVIEW 8(3), 269–274 (2000)

Optimised tapered beam propagation

S. SUJECKI*

National Institute of Telecommunications, 1 Szachowa Str., 04-894 Warsaw, Poland

A novel formulation of tapered beam propagation algorithm is given. The new algorithm is tested on standard taper structures in order to check the accuracy, reciprocity and the convergence rate. It is shown that the new algorithm preserves the advantages of the previous formulation while being easier to implement and requiring less computation per one propagation step. The results obtained by the new algorithm agree with the ones given by the standard rectangular beam propagation method and also fulfil the reciprocity condition to four decimal places of the transmitted power.

Keywords: integrated optics, beam propagation method, finite differences.

1. Introduction

Integrated optics is one of the key technologies needed for the fast development of the transparent optical networks, i.e., optical communication systems which avoid unnecessary conversion between optical and electrical signal (for example during switching).

Due to complicated geometry the design and optimisation of the integrated optics elements results usually in long calculation times and large computer memory requirements. Consequently every modification of the algorithms used, which allows obtaining accurate results faster and using less computer memory, is of great importance.

One of the basic structures, commonly used in integrated optical circuits, is an optical taper [1,2]. The optical tapers are usually utilised to minimise the coupling losses between various light-guiding structures [3]. The standard technique used for the design and optimisation of the optical tapers is the beam propagation method (BPM) [2,4]. This approach can be applied for a wide variety of practically useful structures. Usually BPM is applied in the rectangular coordinate system. As a result the oblique boundaries between core and cladding, which are present in the case of an optical taper, cannot be modelled exactly and must be approximated using staircasing. Consequently an unphysical numerical noise resulting from presence of sudden dielectric discontinuities is observed in the field plots and also influences negatively on accuracy [5]. The only effective way of avoiding this problem, while preserving simple interfacing with standard rectangular BPM, proved to be the application of the beam propagation method in the tapered coordinate system [5,6].

Although there are big advantages of applying BPM in the tapered coordinate system the resulting paraxial wave equation has quite complicated form in comparison with the standard BPM [5,6]. Moreover the Helmholtz equation in the tapered coordinate system contains mixed derivatives, and does not allow variables separation. Thereafter the resulting BPM algorithm has a non-standard form and the only way of introducing the wide-angle scheme was to apply Hadley's recurrent formula [5,7] which, however, is inefficient.

In this paper one-way wave equation in the tapered coordinate system is derived. Then the paraaxial wave equation is given which has particularly simple form. The obtained propagation operator differs only slightly from the one obtained in the rectangular coordinate system and allows the direct utilisation of the sparse matrix representations of the wide angle BPM propagator developed for uni-directional propagation in rectangular coordinate system [8,9].

2. Formulation

Although the tapered coordinate system is not an orthogonal system and therefore does not permit the wave equation to be decomposed by separating the variables the one-way wave equation can be obtained in a similar manner as in the rectangular coordinate system. Not to obscure the idea the derivations are carried out for the 2D TE case only. The TM case derivation can be carried out in a similar manner.

To obtain the one-way wave equation in the tapered coordinate system, it is convenient to start with the wave equation in the rectangular coordinate system x, y, and z

$$\left(\frac{\partial^2}{\partial x^2}+\frac{\partial^2}{\partial z^2}+k^2(x,y,z)\right)\Psi(x,z)=0, \qquad (1)$$

where k is the local wavenumber, given by $n(x,z)\ 2\pi/\lambda_o$, n(x, z) is the y independent refractive index at the operating wavelength λ_o (Fig. 1) and $\psi(x,y,z)$ denotes the y component of the electric field.

*e-mail: S.Sujecki@itl.waw.pl

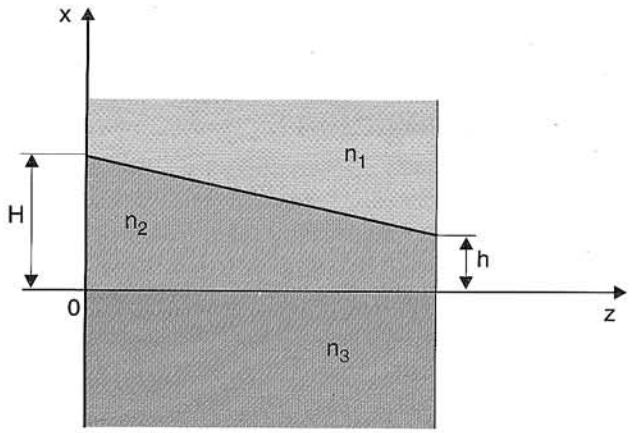

Fig.1. Asymmetric 2D taper structure.

The tapered coordinates t and ζ can be related to x, and z by $x = tz$ and $\zeta = z$.

The derivatives appearing in Eq. (1) can be re-expressed in terms of t and ζ by using the following identities

$$\frac{\partial}{\partial x} = \left(\frac{\partial t}{\partial x}\right)\frac{\partial}{\partial t} + \left(\frac{\partial \zeta}{\partial x}\right)\frac{\partial}{\partial \zeta} = \frac{1}{\zeta}\frac{\partial}{\partial t}$$

$$\frac{\partial}{\partial z} = \left(\frac{\partial t}{\partial z}\right)\frac{\partial}{\partial t} + \left(\frac{\partial \zeta}{\partial z}\right)\frac{\partial}{\partial \zeta} = \frac{\partial}{\partial \zeta} + \frac{t}{\zeta}\frac{\partial}{\partial t}$$

Substituting these expressions into Eq. (1) and rearranging gives

$$\left(\frac{\partial}{\partial \zeta} + \frac{t}{\zeta}\frac{\partial}{\partial t}\right)^2 \psi(t,\zeta) = \left(\frac{1}{\zeta^2}\frac{\partial^2}{\partial t^2} + k^2 + \beta^2 - \beta^2\right)\psi(t,\zeta), \qquad (2)$$

where β is a reference propagation constant. Expressing the Helmholtz equation in the tapered coordinate system in the form of Eq. (2) is the key point of this derivation as it follows that the one-way wave equation can be expressed as

$$\left(\frac{\partial}{\partial \zeta} + \frac{t}{\zeta}\frac{\partial}{\partial t}\right)\psi(t,\zeta) = \pm j\sqrt{\beta^2 + L}\,\psi(t,\zeta), \qquad (3)$$

where the operator L

$$L = \frac{1}{\zeta^2}\frac{\partial^2}{\partial t^2} + k^2 - \beta^2.$$

It can also be noted that the square root operator does not differ from the one, which is obtained in the rectangular coordinate system. Consequently the sparse matrix representations, which are optimised for the suppression of the evanescent waves, developed in acoustics [8] and optics [9] can be utilised directly.

The paraxial BPM can be now obtained approximating the square root operator using a truncated (after the second term) Taylor series expansion. After having introduced the envelope function – $\psi(\zeta,z) = \varphi(\zeta,z)\exp(\pm j\beta z)$ the paraxial wave equation in the tapered coordinate system is obtained

$$\frac{\partial}{\partial \zeta}\varphi(t,\zeta) = \left(-\frac{t}{\zeta}\frac{\partial}{\partial t} \pm j\frac{1}{2\beta}L\right)\varphi(t,\zeta). \qquad (4)$$

The higher order approximations of the square root operator can be easily introduced analogously to the standard rectangular BPM. The guidelines for a suitable choice of β can be found for example in Refs. 2 and 5. The form of the obtained paraxial wave equation is much simpler than the one presented in Refs. 5 and 6. It differes only from the rectangular coordinate case by the presence of the term $t/\zeta\,\partial/\partial t$. Consequently extension of the standard rectangular BPM to the tapered one becomes now a minor correction and the additional computations required are reduced.

The right hand side (RHS) operator in Eq. (4) can now be discretised using finite difference (FD) method. The resulting matrix equation can be solved using a Crank-Nicholson scheme. Denoting the RHS operator of Eq. (4) as $M = A + B$, where

$$A = -\frac{t}{\zeta}\frac{\partial}{\partial t}, \quad B = \pm j\frac{1}{2\beta}L$$

we obtain

$$\varphi(t,\zeta+\Delta\zeta) = \frac{1 + \frac{1}{2}\Delta\zeta(A^d \pm B^d)}{1 - \frac{1}{2}\Delta\zeta(A^d \mp B^d)}\varphi(t,\zeta), \qquad (5)$$

where the superscript d denotes the FD discretised counterpart of a respective differential operator. Equation (5) can be handled using a standard tridiagonal matrix solver [5]. At the boundary of the analysis window a transparent boundary condition is assumed [10].

3. Results and discussion

In order to verify the convergence rate, accuracy and reciprocity the results obtained are compared with quite recently published benchmark results [11]. The structures studied are an asymmetric air clad and a semiconductor clad taper (Fig. 1). The air clad taper is decreased from a width of 0.8–0.4 μm over a distance of either 22.9 μm or 229 μm. The semiconductor clad taper is tapered from the width of 0.2–0.1 μm over a distance of either 5.73 μm or 57.3 μm.

In Figs. 2(a)–2(d) the dependence of the power content guided in the fundamental TE mode measured at the end of the taper on the transverse mesh size is shown. In order to fulfil the reciprocity condition the power transfer between

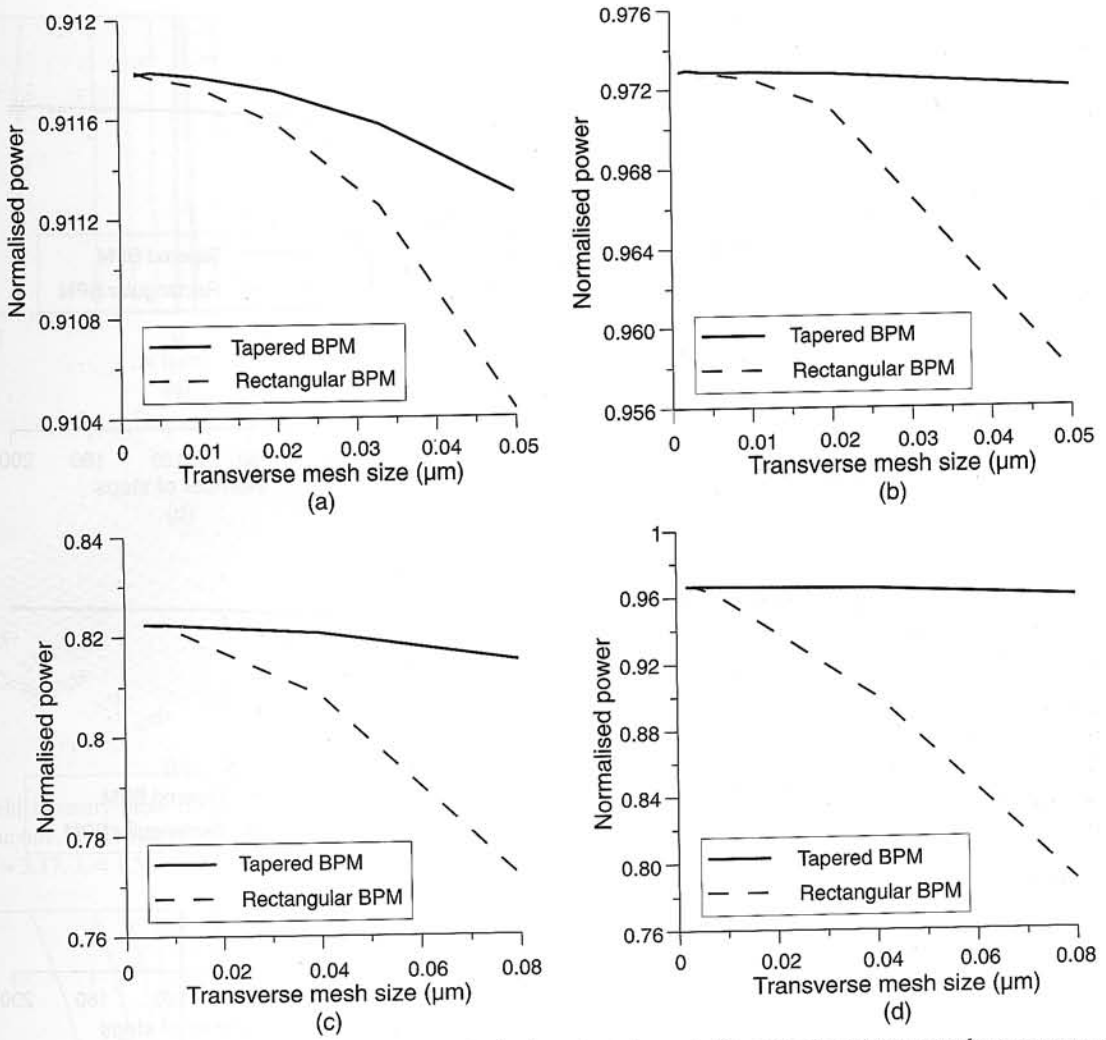

Fig. 2. Dependence of power content in fundamental x-polarised mode at the end of a symmetrical taper on the transverse mesh size;
(a) H = 0.2 μm, h = 0.1 μm, L = 5.73 μm, $n_1 = 3.17$, $n_2 = 3.3$, $n_3 = 3.17$, $\lambda = 1.55$ μm
(b) H = 0.2 μm, h = 0.1 μm, L = 57.3 μm, $n_1 = 3.17$, $n_2 = 3.3$, $n_3 = 3.17$, $\lambda = 1.55$ μm
(c) H = 0.8 μm, h = 0.4 μm, L = 22.9 μm, $n_1 = 1.00$, $n_2 = 3.3$, $n_3 = 3.17$, $\lambda = 1.55$ μm
(d) H = 0.8 μm, h = 0.4 μm, L = 229 μm, $n_1 = 1.00$, $n_2 = 3.3$, $n_3 = 3.17$, $\lambda = 1.55$ μm

input and output has been calculated using $\int_{-\infty}^{+\infty} |E|^2 \, dx$ as conserved quantity [11]. It was also assumed that the initial field distribution corresponds to the local fundamental mode. As can be seen the results obtained applying the finite difference beam propagation method in the tapered coordinate system (tapered FD-BPM) converge much faster than in the case of the finite difference beam propagation method in the rectangular coordinate system (rectangular FD-BPM). Consequently, the desired accuracy can be obtained using smaller matrices, which results in relaxing the memory requirement and decreasing the calculation time. Moreover, it is noted that the advantage of applying the tapered FD-BPM is especially pronounced in the case of strongly guiding structures, i.e., Figs. 2(c) and 2(d).

In Figs 3(a)–3(d) the dependence of the power content in the fundamental TE mode measured at the end of the taper on the number of steps needed by a BPM algorithm to calculate the output field profile is shown. As it can be seen, the results obtained applying the tapered FD-BPM converge usually faster or at a similar rate as in the case of the rectangular FD-BPM.

In Figs. 4–7 the intensity distributions of the y component of the electric field are given. The results presented are normalised with respect to the maximum field intensity of the input field distribution. In the contour plots the lines of constant field intensity are given starting at 0.1 of the maximum value with an increment of 0.2. It is noticed that for the semiconductor clad structure with the length of 5.73 μm the contours are almost the straight lines, Fig. 4, as if the guided light was not following the taper structure. Consequently the circular wave fronts observed typically in tapers [12] are not present here. Thereafter for this particular structure the advantages of applying the tapered coordinate system are smaller as it is indicated also by the results depicted espe-

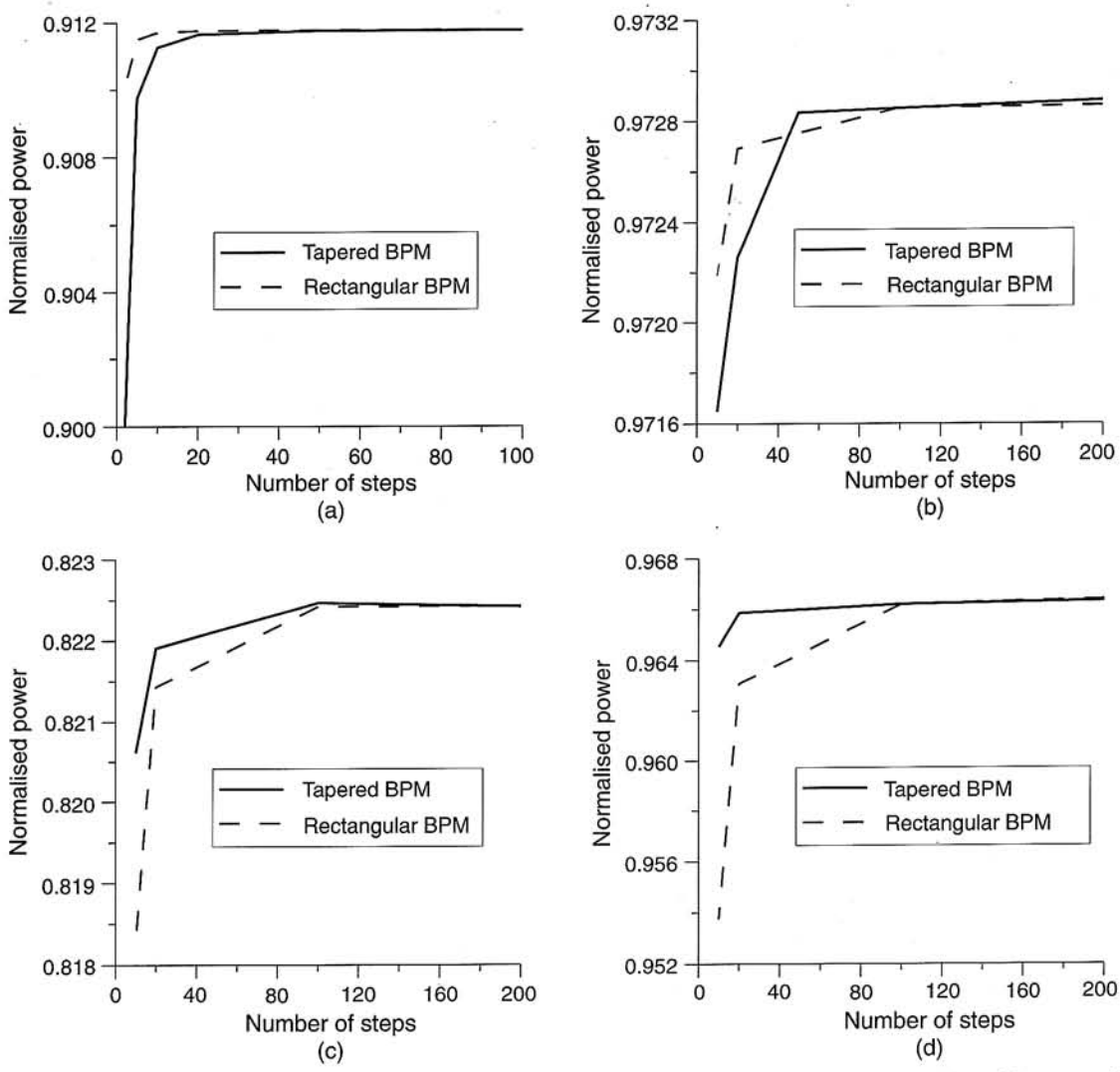

Fig. 3. Dependence of power content in fundamental x-polarised mode at the end of a symmetrical taper on the number of the propagation steps,
(a) H = 0.2 μm, h = 0.1 μm, L = 5.73 μm, n_1 = 3.17, n_2 = 3.3, n_3 = 3.17, λ = 1.55 μm
(b) H = 0.2 μm, h = 0.1 μm, L = 57.3 μm, n_1 = 3.17, n_2 = 3.3, n_3 = 3.17, λ = 1.55 μm
(c) H = 0.8 μm, h = 0.4 μm, L = 22.9 μm, n_1 = 1.00, n_2 = 3.3, n_3 = 3.17, λ = 1.55 μm
(b) H = 0.8 μm, h = 0.4 μm, L = 229 μm, n_1 = 1.00, n_2 = 3.3, n_3 = 3.17, λ = 1.55 μm

Table 1: Power content in the fundamental TE mode at the and of the tapers: Air: W_i = 0.8 μm, W_o = 0.4 μm, n_f = 3.3, n_s = 3.17, n_c = 1.0, 1° : L = 22.9 μm, 0.1° : L = 229 μm; Semi: W_i = 0.2 μm, W_o = 0.1 μm, n_f = 3.3, n_s = 3.17, n_c = 3.17, 1° : L = 5.73 m, 0.1° : L = 57.3 μm.

	Air: 1° forward (%)	Air: 1° backward (%)	Air: 0.1° forward (%)	Air: 0.1° backward (%)	Semi: 1° forward (%)	Semi: 1° backward (%)	Semi: 0.1° forward (%)	Semi: 0.1° backward (%)
Twente*	82.30	82.30	96.81	96.64	91.18	91.19	97.32	97.30
Porto*	82.20	82.40	96.70	96.60	91.19	91.19	97.31	97.30
Hagen*	81.50	81.40	96.36	96.36	91.19	91.19	97.28	97.28
HHI*	81.60	81.50	96.70	96.50	91.10	91.20	97.50	97.50
Thomson*	82.10	82.30	96.54	96.61	91.18	91.18	97.28	97.27
Tapered°	82.24	82.24	96.63	96.63	91.18	91.18	97.29	97.29
Rectangular°	82.24	82.24	96.63	96.63	91.18	91.18	97.29	97.29

*Results publishd in Ref. 11.
°Results obtained by the author.

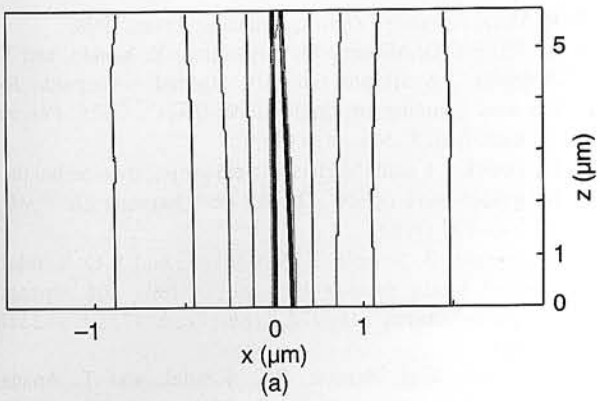

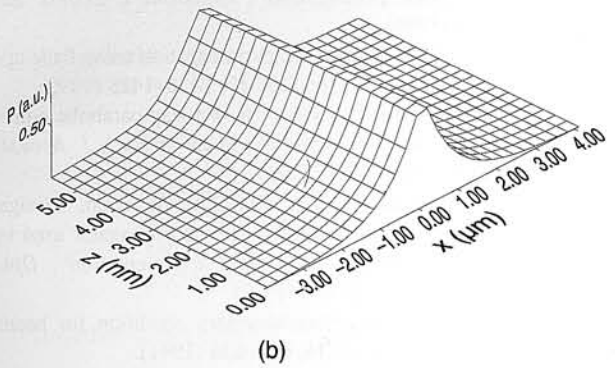

Fig. 4. Field intensity plots for x-polarised case in symmetrical tapered structure. H = 0.2 μm, h = 0.1 μm, L = 5.73 μm, n_1 = 3.17, n_2 = 3.3, n_3 = 3.17, λ = 1.55 μm (a) contour plot, (b) surface plot.

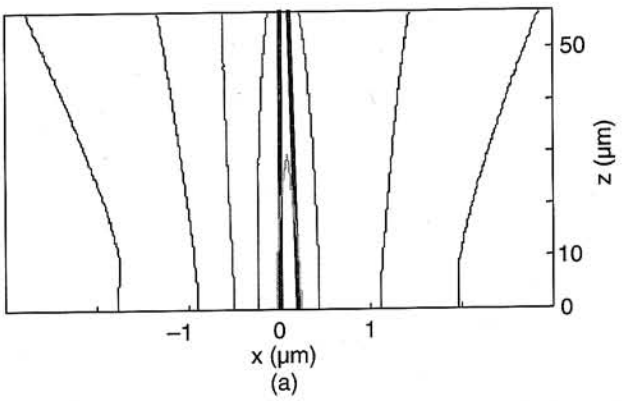

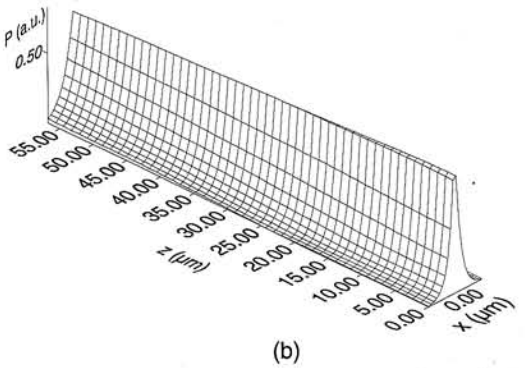

Fig. 5. Field intensity plots for x-polarised case in symmetrical tapered structure. H = 0.2 μm, h = 0.1 μm, L = 57.3 μm, n_1 = 3.17, n_2 = 3.3, n_3 = 3.17, λ = 1.55 μm (a) contour plot, (b) surface plot.

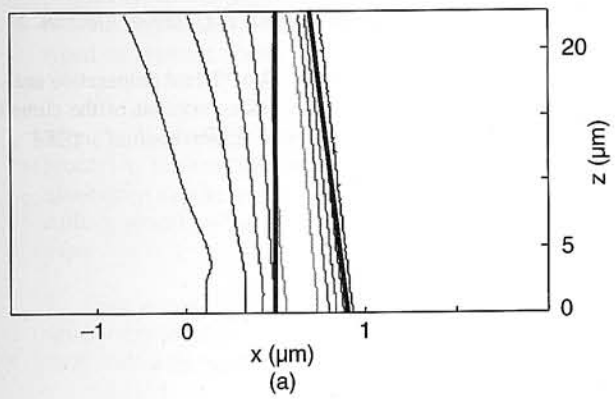

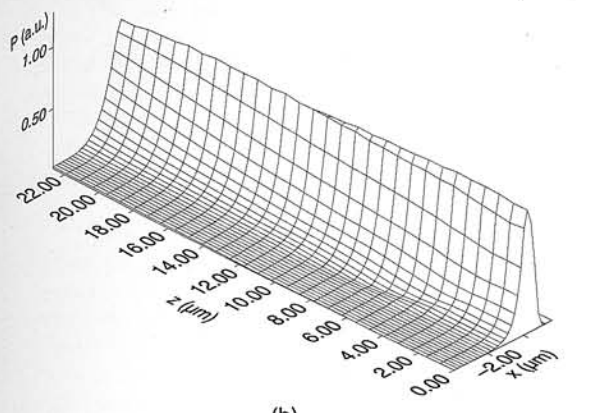

Fig. 6. Field intensity plots for x-polarised case in symmetrical tapered structure. H = 0.8 μm, h = 0.4 μm, L = 22.9 μm, n_1 = 1, n_2 = 3.3, n_3 = 3.17, λ = 1.55 μm (a) contour plot, (b) surface plot

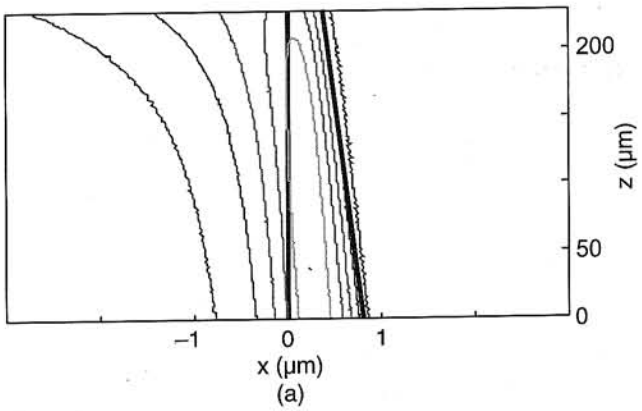

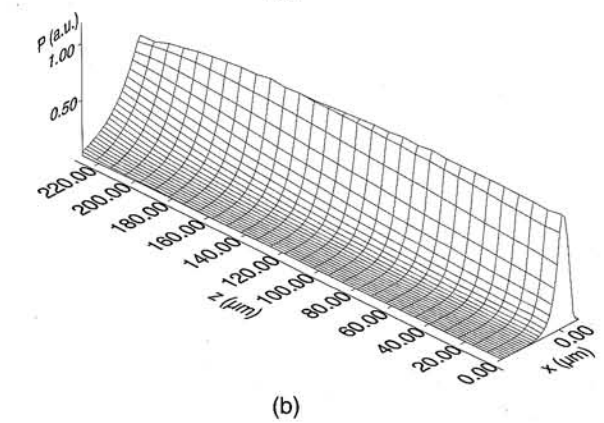

Fig. 7. Field intensity plots for x-polarised case in symmetrical tapered structure. H = 0.8 μm, h = 0.4 μm, L = 229 μm, n_1 = 1, n_2 = 3.3, n_3 = 3.17, λ = 1.55 μm (a) contour plot, (b) surface plot.

cially in Fig. 3(a). However, if the wave fronts indicate typical circular character, namely in the case of strongly guiding structures, the tapered FD-BPM is by far superior to the rectangular one [Figs. 2(c) and 2(d) and Figs. 3(c) and 3(d)].

In Table 1 the power content in the fundamental TE mode measured at the end of the taper is given. A good agreement is generally observed with other authors. It is also noticed that the results obtained by the author using tapered FD-BPM and rectangular FD-BPM agree to the fourth decimal place and also indicate reciprocity on four digits. To the best knowledge of the author such agreement obtained using two independent BPM approaches is reported for the first time. The results obtained by the author indicate also that the larger discrepances with the results obtained by other authors can be explained by the fact that they were not using sufficiently fine finite difference meshes.

4. Conclusions

A new formulation of the tapered finite difference beam propagation method in the tapered coordinate system is given. The results obtained confirm that the new algorithm preserves the advantages of the previous formulation while being easier to implement and faster.

A four digit agreement is observed between the results calculated be the two independent BPM methods, namely tapered and rectangular FD-BPM. To the best knowledge of the author such agreement is reported for the first time in the literature.

References

1. K.J Ebeling, *Integrated Optoelectronics*, Springer-Verlag, 1993.
2. R. März, *Integrated Optics*, Academic Press, 1998.
3. K. Kasaya, O. Mitomi, M. Naganuma, Y. Kondo, and Y. Noguchi, "A simple laterally tapered waveguide for low-loss coupling to single-mode fibres", *IEEE Photon. Technol. Lett.* **5**, 345–347 (1993).
4. D. Yevick, "A guide to electric field propagation techniques for guided-wave optics", *Optical and Quantum Electronics* **26**, 185–197 (1994).
5. S. Sujecki, P. Sewell, T.M. Benson, and P.C. Kendal, "Novel beam propagation algorithms for tapered optical structures", *IEEE J. Light. Tech.* **17**, 2379–2388 (1999).
6. P. Sewell, T.M. Benson, P.C. Kendal, and T. Anada, "Tapered beam propagation", *Electronics Letters* **32**, 1025–1026 (1996).
7. G.R. Hadley, "Wide angle beam propagation using Pade approximant operators", *Opt. Lett.* **17**, 1426–1428 (1992).
8. M.D. Collins and R.D. Evans, "A two-way parabolic equation for acoustic back scattering in the ocean", *J. Acoust. Soc. Am.* **91**, 1357–1368 (1992).
9. M.J.N. Van Stralen, H. Blok, and M.V. De Hoop, "Design of sparse matrix representations for the propagator used in BPM and directional wave field representation", *Opt. Quant. Electr.* **29**, 179–198 (1997).
10. G.R. Hadley, "Transparent boundary condition for beam propagation", *Opt. Lett.* **16**, 624–626 (1991).
11. J. Haes *et al.*, "A comparison between different propagative schemes for the simulation of tapered step index slab waveguides", *IEEE J. Light. Techn.* **14**, 1557–1567 (1996).
12. M. Cada, F. Xiang, and L.B. Felsen, "Intrinsic modes in tapered optical waveguides", *IEEE J. Quantum Electron.* **24**, 758–765 (1988).
13. C.T. Lee, M.L. Wu, and J.M. Hsu, "Beam propagation analysis for tapered waveguides: taking account of the curved phase-front effect in paraxial approximation", *IEEE J. Light. Techn.* **15**, 2183–2189 (1997).

